



This is a repository copy of *Detecting noise with shot noise using on-chip photon detector*.

White Rose Research Online URL for this paper:
<http://eprints.whiterose.ac.uk/87856/>

Version: Accepted Version

Article:

Jompol, Y., Roulleau, P., Jullien, T. et al. (4 more authors) (2015) Detecting noise with shot noise using on-chip photon detector. *Nature Communications*, 6. 6130. ISSN 2041-1723

<https://doi.org/10.1038/ncomms7130>

Reuse

Unless indicated otherwise, fulltext items are protected by copyright with all rights reserved. The copyright exception in section 29 of the Copyright, Designs and Patents Act 1988 allows the making of a single copy solely for the purpose of non-commercial research or private study within the limits of fair dealing. The publisher or other rights-holder may allow further reproduction and re-use of this version - refer to the White Rose Research Online record for this item. Where records identify the publisher as the copyright holder, users can verify any specific terms of use on the publisher's website.

Takedown

If you consider content in White Rose Research Online to be in breach of UK law, please notify us by emailing eprints@whiterose.ac.uk including the URL of the record and the reason for the withdrawal request.



eprints@whiterose.ac.uk
<https://eprints.whiterose.ac.uk/>

Detecting noise with shot noise: a new on-chip photon detector

Y. Jompol^{1,*,\dagger}, P. Roulleau^{1,*}, T. Jullien¹, B. Roche¹, I. Farrer²,
D.A. Ritchie², and D. C. Glattli¹

¹Nanoelectronics Group, Service de Physique de l'Etat Condense,
IRAMIS/DSM (CNRS URA 2464), CEA Saclay, F-91191 Gif-sur-Yvette,
France

²Cavendish Laboratory, University of Cambridge, J.J. Thomson Avenue,
Cambridge CB3 0HE, UK

The high frequency radiation emitted by a quantum conductor presents a rising interest in quantum physics and condensed matter [1, 6, 3, 4, 5, 7, 8]. However its detection with microwave circuits is challenging. The important mismatch between the quantum conductor impedance ($\sim h/e^2$) and the circuit impedance (typically 50Ω) strongly limits the sensitivity. Recent realization of on-chip quantum detection [7, 9, 10, 11, 12, 13] have circumvented this issue using spatially close detectors with larger impedance providing high sensitivity up to high frequency. However, they lack of a universal photon-response. Here, we propose to use the Photon-Assisted Shot Noise (PASN) for on-chip radiation detection. It is based on the low frequency current noise generated by the partitioning of photon excited electrons and holes which are scattered inside the conductor [14, 15, 16, 17]. For a given electromagnetic coupling to the radiation, the PASN response is independent on the nature and geometry of the quantum conductor used for the detection, up to a Fano factor, characterizing the type of scattering mechanism. Ordered in temperature/frequency range, from few tens of milli-Kelvin/GHz to several hundreds of Kelvin/THz, a wide variety of conductors can be used like Quantum Point Contacts (this work), diffusive metallic or semi-conducting films, Graphene, Carbon nanotubes and even molecule, opening new experimental opportunities in quantum physics.

To circumvent impedance mismatch limitation, different types of on-chip photon detectors have been developed using a second nearby quantum conductor and exploiting its photon detection ability. On-chip detectors have been realized using GaAs/AlGaAs 2D electron gas patterned quantum dots [9, 10] and Aluminium or Niobium SIS junctions [11, 12, 13, 7]. The photon-response of quantum dots depends on an energy scale set by their geometry, that of superconducting junctions is limited by a characteristic energy gap and both systems show tunnel resistance variability. Regarding bolometric detectors their efficiency depends on the phonon relaxation time, requires low temperature and shows slow response time.

In this letter, we propose a novel on-chip radiation detection based on PASN. When a quantum conductor is submitted to a time dependent drain-source voltage, electrons and holes are created which then scatter inside the conductor. Their partitioning between source and drain contacts leads to a current noise called Photo-Assisted Shot Noise. Remarkably, there is a simple link between PASN and the incident radiation power up to a noise Fano factor characterizing the statistics of partitioning. This simple link is better understood if we remark that PASN is the quantum manifestation of the rectification property of ordinary shot noise [18, 19, 20, 21] which is proportional to the absolute value of the drain-source voltage.

Figure 1 shows the principle of the on-chip detection. It consists of two separate excitation and measurement circuit lines etched in a high mobility two-dimensional electron gas (2DEG). Each line involves two QPCs in se-

ries. On the upper line, the left QPC is the high-frequency emitter. When biased by the dc voltage V_{ds}^E it generates shot noise up to the frequency eV_{ds}^E/h [20, 22]. The right QPC tuned on a conductance plateau acts as a stable series resistance R_S^E converting current noise into voltage noise. In the lower line the left QPC is the detector. In series with the right QPC, also tuned on a resistance plateau R_S^D , it experiences the emitter line voltage fluctuations via the coupling capacitance C_C up to the cut-off frequency f_{max} [23]. The number of electron-hole pairs generated in the detector line is a direct function of the radiated noise power integrated up to frequency $\min(eV_{ds}^E/h, f_{max})$. Their scattering by the QPC detector generates a low-frequency PASN which is measured. f_{max} depends on all QPC resistances and on the self-capacitance C_{self} of the 2DEG part between the QPCs in series.

To understand the photon detection principle, let us first assume that the detector line is excited by a coherent radiation at frequency $\Omega/2\pi$ such that $V_{ds}^E(t) = V_{ac} \cos(\Omega t)$. Electrons in the detector line can absorb l photons of energy $E_l = l\hbar\Omega$ by creating an electron-hole pair with a probability $P(E_l) = |J_l(eV_{ac}/\hbar\Omega)|^2$, with J_l the l^{th} Bessel function. Electrons and holes are independently and randomly partitioned by the QPC detector between left and right contacts. This generates a PASN whose low-frequency spectral density of current fluctuations S_I^{PASN} is given by [14, 15, 16, 17]:

$$S_I^{PASN} = \frac{2e^2}{h} [4k_B T_e \sum_n D_{D,n}^2 + 2 \sum_n D_{D,n} (1 - D_{D,n}) \sum_{l=-\infty}^{l=+\infty} E_l P(E_l) \coth \frac{E_l}{2k_B T_e}] \quad (1)$$

with T_e the electronic temperature and $D_{D,n}$ the transmission of the n^{th} electronic mode through the detector QPC, $n=1, 2, \dots$. For weak ac voltage $eV_{ac} \ll \hbar\Omega$ and zero temperature a direct relation can be established between the radiation power $P_{rad} = V_{ac}^2/2Z_{rad}$ and the current noise: $S_I^{PASN} \simeq 2G_D F(Z_{rad}e^2/\hbar)P_{rad}/\Omega$, where Z_{rad} is the radiation impedance assumed smaller than the QPC detector conductance G_D and F the Fano factor.

From Eq. (1), it is clear that the maximum PASN will be obtained for total transmission $D_D = \sum_n D_{D,n} = k + 1/2$, k an integer. In addition to shot noise, a photon assisted dc current I_{ph} is generated when considering the (weak) energy dependence of the QPC transmission :

$$I_{ph} = \frac{2e}{h} \int d\epsilon \left(-\frac{\partial f}{\partial \epsilon}\right) \left(\sum_n \frac{\partial D_{D,n}}{\partial \epsilon}\right) \sum_{l=-\infty}^{l=+\infty} E_l^2 P(E_l) \quad (2)$$

$f(\epsilon)$ is the equilibrium Fermi distribution. Modeling the QPC transmission with a saddle point potential [24, 25], it can be shown that $\frac{\partial D_{D,n}}{\partial \epsilon} \propto D_{D,n}(1 - D_{D,n})$: maximum photocurrents will be also obtained at half-integer D_D .

In the present case, the excitation is not coherent but due to random fluctuations of the QPC detector drain-source voltage which originates from the capacitive coupling with the noisy QPC emitter. The above expressions can be generalized, giving the PASN as:

$$S_I^{PASN} = \frac{2e^2}{h} [4k_B T_e \sum_n D_{D,n}^2 + 2 \sum_n D_{D,n} (1 - D_{D,n}) \int EP(E) \coth \frac{E}{2k_B T_e} dE] \quad (3)$$

and the photocurrent:

$$I_{ph} = \frac{2e}{h} \int d\epsilon \left(-\frac{\partial f}{\partial \epsilon} \right) \left(\sum_n \frac{\partial D_{D,n}}{\partial \epsilon} \right) \int E^2 P(E) dE \quad (4)$$

The generalized probability distribution $P(E)$ is similar to the $P(E)$ function used in the dynamical Coulomb blockade theory (see Supplementary Information). It is a direct function of the radiation power to be detected, which as a shot noise itself is maximum for $D_E = 0.5$.

We first focus on the photocurrent whose measurement set-up is described in Fig. 2(a). Source V_{in} leads to a current in the upper line and to the voltage difference V_{ds}^E across the emitter. The resulting shot noise induces a photocurrent I_{ph} in the detector. We modulate V_{in} at frequency 174 Hz and detect the induced photocurrent using lock-in techniques. Series resistances are tuned on a plateau for each line while the emitter and detector

transmissions are varied. Following the saddle point potential model of a QPC [24, 25], the transmission of the n^{th} mode can be written $D_{D,n}(V_g) = 1/(1+e^{2\pi(V_0-V_g)/V_{g,n}})$ where $V_{g,n}$ is related to the negative curvature of the saddle point potential. The photocurrent is given by (see Supplementary Information):

$$I_{ph} = \frac{e}{h} \frac{1}{\Delta} \frac{k_B T_E^* e^2}{C_{\text{self}}} \sum_n \frac{2\pi}{V_{g,n}} D_{D,n} (1 - D_{D,n}) \quad (5)$$

$V_{g,n}$ and the lever arm $\Delta = \partial\epsilon/\partial V_g$ are extracted from a study of the differential QPC conductance versus gate and bias voltages. We have introduced T_E^* as the effective noise temperature of the circuit which, up to a coupling factor, includes a combination of the shot noise temperature of the emitter: $(1 - D_E) \frac{eV_E}{2k_B}$ plus other equilibrium thermal noise contributions of the circuit surrounding the detector QPC (see the supplementary Information).

The color plot in Fig. 2(b) shows the measured photocurrent as a function of the emitter and detector transmissions D_E and D_D , up to two transmitting orbital electronic modes. Above the color plot, the photocurrent is plotted as a function of D_D for a fixed value of $D_E \sim 0.45$. As expected, it is maximum for half transmission of the emitter electronic modes and vanishes for integer transmission. These measurements have been found essential for a fine calibration of the electrical circuit and for complementary characterization of the photon-assisted shot noise effect (see the Supplementary Information).

We now consider PASN measurements. The cross correlation noise measurement set up is described in Fig. 3(a). To characterize the detector line, the QPC detector transmission is set to $D_D = 0.5$ while a dc bias is applied on the detector line. The resulting shot noise measured, black dots in Fig. 3(b), perfectly agrees with the theory in red solid line. We extract an electronic temperature $T_e = 310$ mK close to the fridge temperature $T = 300$ mK. Then we turn off the applied bias on the detector line and the QPC emitter is biased and also tuned at transmission $D_E = 0.5$. Both series resistances are tuned on the first plateau. Because of the coupling capacitance, voltage fluctuations are reported on the detector line. The only dc current flowing through the detector line being the weak dc photocurrent, no detectable transport shot noise is expected. However, we detect some noise, confirming that the PASN detection works as illustrated in Fig. 3(c), black circle. The detected PASN, $\Delta S_I^{PASN,D}$, is expected to be:

$$\Delta S_I^{PASN,D} \simeq -\frac{4e^2}{h} D_D (1 - D_D) \frac{e^2}{C_{self}} \frac{T_E^*}{6T_e} \quad (6)$$

Here, considering $P(E)$ takes only important values for $E \ll k_B T_e$, a low-energy expansion of Eq. (3) has been made. The $T_E^*(V_{ds}^E)/C_{self}$ amplitude compatible with the detector geometry (estimated $C_{self}=3$ fF and $C_c=1$ fF) and obtained from photocurrent measurements can now be compared to the noise measurement. The theoretical prediction (red solid line) following Eq. 6 also includes an additional term due to heating effect. We discuss this

point in the following.

We open the series QPC of the detector line such that the current to voltage fluctuation conversion is now mediated by the smaller resistance of the long resistive mesa. Then we apply a fixed bias V_{ds}^D and sweep the detector transmission (red circles in Fig. 4(a)). As expected the shot noise is maximum for $D_D = 0.5$ and cancels for $D_D = 1$. The slight disagreement with the theoretical prediction (red solid line) around $D_D \sim 0.7$ reveals a weak "0.7" anomaly [26, 27, 28, 29]. Then we tune the series QPC on its first plateau and repeat the same experiment (black circles). Surprisingly, the shot noise does not cancel anymore for $D_D = 1$. To understand it, we must consider heating effects. Since the size of the QPC is much smaller than the electron-phonon relaxation length, there is a temperature gradient from the QPC to the ohmic contacts assumed to be at the base temperature of the fridge. Combining Joule heating together with the Wiedemann-Franz law, we obtain [18]:

$$T_e(V_{ds}) = T_{fridge}^2 + \frac{24}{\pi^2} \frac{G}{G_m} \left(1 + \frac{2G}{G_m}\right) \left(\frac{eV_{ds}}{2k_B}\right)^2 \quad (7)$$

with G_m the total conductance linking the QPC to the ohmic contacts, and T_{fridge} the base temperature. Considering this effect, a QPC tuned on a plateau will not be noiseless anymore. We find a good agreement with measurements, black solid line.

We now apply $V_{ds}^E=6$ mV on the emitter line, fixing $D_E \sim 0.5$ to get the maximum emitted signal. In Fig. 4(b), the PASN is measured as a function of D_D . The non zero value of the shot noise for $D_D = 1$ results from the similar heating effect. The agreement between theory and experimental data confirms our good understanding of the "on-chip" detection mechanism: *both photocurrent and PASN result from the same photon assisted effect.*

To conclude, we have described a new way of detecting high frequency voltage fluctuations based on photon-assisted shot noise measurement and seconded by photocurrent measurement. If the latter depends on the details of the mesoscopic conductor used, PASN is universal up to a noise Fano factor. The PASN approach for noise or photon radiation detection can be applied to other systems. This technique offers the possibility to probe mesoscopic properties at very high frequency (GHz and THz) of various materials (GaAs, Graphene, Carbon nanotube).

Methods

Emitter and detector lines were patterned using e-beam lithography on a high mobility two dimensional electron gas formed at the GaAs/ $Ga_xAl_{1-x}As$ heterojunction. The two-dimensional electron gas is constituted 100nm below the surface has a density of $1.8 \times 10^{11} \text{ cm}^{-2}$ and mobility $2.69 \times 10^6 \text{ cm}^2/\text{V s}$. Measurements were performed in cryogen free ^3He cryostat at 300 mK (base temperature).

References

- [1] Aguado, R., & Kouwenhoven L., P., Double Quantum Dots as Detectors of High-Frequency Quantum Noise in Mesoscopic Conductors, *Phys. Rev. Lett.* **84**, 1986 (2000)
- [2] Zazunov, A., Creux, M., Paladino, E., Crpieux, A., and Martin T., Detection of Finite-Frequency Current Moments with a Dissipative Resonant Circuit, *Phys. Rev. Lett.* **99**, 066601 (2007)
- [3] Beenakker, C. W. J. & Schomerus, H., Antibunched photons emitted by a quantum point contact out of equilibrium. *Phys. Rev. Lett.* **93**, 096801 (2004).
- [4] Zakka-Bajjani, E., Dufouleur, J., Coulombel, N., Roche, P., Glattli, D., C., and Portier, F., Experimental Determination of the Statistics of Photons Emitted by a Tunnel Junction, *Phys. Rev. Lett.* **104**, 206802 (2010)
- [5] Trauzettel, B., Safi, I., Dolcini, F., and Grabert, H., Appearance of fractional charge in the noise of non-chiral Luttinger liquids, *Phys. Rev. Lett.* **92**, p. 226405 (2004)
- [6] Zazunov, A., Creux, M., Paladino, E., Crpieux, A., and Martin T., Detection of Finite-Frequency Current Moments with a Dissipative Resonant Circuit, *Phys. Rev. Lett.* **99**, 066601 (2007)

- [7] Basset, J., Kasumov, A., Y., Moca, C., P., Zaránd, G., Simon, P., Bouchiat, H., and Deblock, J. Measurement of Quantum Noise in a Carbon Nanotube Quantum Dot in the Kondo Regime, *Phys. Rev. Lett.* **108**, 046802 (2012)
- [8] Delbecq, M., R., et al., Coupling a Quantum Dot, Fermionic Leads, and a Microwave Cavity on a Chip, *Phys. Rev. Lett.* **107**, 256804 (2011)
- [9] Gustavsson, S., et al, Frequency-Selective Single-Photon Detection Using a Double Quantum Dot *Phys. Rev. Lett.*, **99** 206804 (2007).
- [10] E. Onac, et al, Using a Quantum Dot as a High-Frequency Shot Noise Detector, *Phys. Rev. Lett.*, **96** 176601, (2006).
- [11] Deblock, R., Onac, E., Gurevich, L., and Kouwenhoven, L., P., Detection of Quantum Noise from an Electrically Driven Two-Level System *Science*, **301** 203, (2003).
- [12] Billangeon, P., M., Pierre, F., Bouchiat, H., and Deblock, R., Emission and Absorption Asymmetry in the Quantum Noise of a Josephson Junction *Phys. Rev. Lett.*, **96** 136804, (2006).
- [13] Basset, J., Bouchiat, H., and Deblock, R., Emission and Absorption Quantum Noise Measurement with an On-Chip Resonant Circuit *Phys. Rev. Lett.*, **105** 166801, (2010).
- [14] Lesovik, G., B., and Levitov, L., S., Noise in an ac biased junction: Nonstationary Aharonov-Bohm effect *Phys. Rev. Lett.*, **72** 538, (1994).

- [15] M.H. Pedersen and M. Büttiker, *Phys. Rev. B*, **58** 12993, (1998).
- [16] Schoelkopf, R., J., Kozhevnikov, A., A., Prober, D., E., and Rooks, M., J., Observation of Photon-Assisted Shot Noise in a Phase-Coherent Conductor *Phys. Rev. Lett.*, **80** 2437, (1998).
- [17] Reydellet, L.-H., Roche, P., Glattli, D., C., Etienne, B., and Jin, Y., Quantum Partition Noise of Photon-Created Electron-Hole Pairs *Phys. Rev. Lett.*, **90** 176803, (2003).
- [18] Kumar, A., Saminadayar, L., Glattli, D., C., Jin, Y., and Etienne, B., Experimental Test of the Quantum Shot Noise Reduction Theory *Phys. Rev. Lett.*, **76** 2778, (1996).
- [19] Reznikov, M., Heiblum, M., Shtrikman, H., and Mahalu, D., Temporal Correlation of Electrons: Suppression of Shot Noise in a Ballistic Quantum Point Contact, *Phys. Rev. Lett.*, **75** 3340, (1995).
- [20] Lesovik, G., B., Excess quantum noise in 2D ballistic point contacts *JETP Lett.*, **49** 594, (1989).
- [21] Blanter, Y., M., and Büttiker, M., Shot noise in mesoscopic conductors *Phys. Rep.*, **336** 1, (2000).
- [22] E. Zakka-Bajjani, et al, Experimental Test of the High-Frequency Quantum Shot Noise Theory in a Quantum Point Contact *Phys. Rev. Lett.*, **99** 236803, (2007).

- [23] Hashisaka, M., et *al*, Bolometric detection of quantum shot noise in coupled mesoscopic systems *Phys. Rev. B*, **78** 241303(R), (2008).
- [24] M. Büttiker, Quantized transmission of a saddle-point constriction *Phys. Rev. B*, **41** 7906(R), (1990).
- [25] Kemple, E., C., A Contribution to the Theory of the B. W. K. Method *Phys. Rev.*, **48** 549, (1938).
- [26] Thomas, K., J., et *al*, Possible Spin Polarization in a One-Dimensional Electron Gas *Phys. Rev. Lett.*, **77** 135, (1996).
- [27] Roche, P. et *al*, Fano Factor Reduction on the 0.7 Conductance Structure of a Ballistic One-Dimensional Wire, *Phys. Rev. Lett.*, **93** 116602, (2004).
- [28] Reilly, D., J., Zhang, Y., and DiCarlo, L., Phenomenology of the 0.7 conductance feature *Physica E*, **34** 27, (2006).
- [29] DiCarlo, L., et *al*, Shot-noise signatures of 0.7 structure and spin in a quantum point contact *Phys. Rev. Lett.*, **97** 036810, (2006).

Acknowledgement

The ERC Advanced Grant 228273 is acknowledged. The authors are grateful to P. Jacques for experimental support.

Author Contributions

* both authors contributed equally

†Present address: Department of Physics, Mahidol University, Thailand

D.C.G. designed the project. Y.J., P.R., T.J., B.R. performed experiments, analyzed data and wrote the manuscript. P.R., D.C.G. wrote the manuscript Y.J., P.R. set up the measurement system. Y.J. fabricated the sample. I.F. and D.A. Ritchie grew the wafer.

Competing interests statement

The authors declare that they have no competing financial interests.

Supplementary Information is available

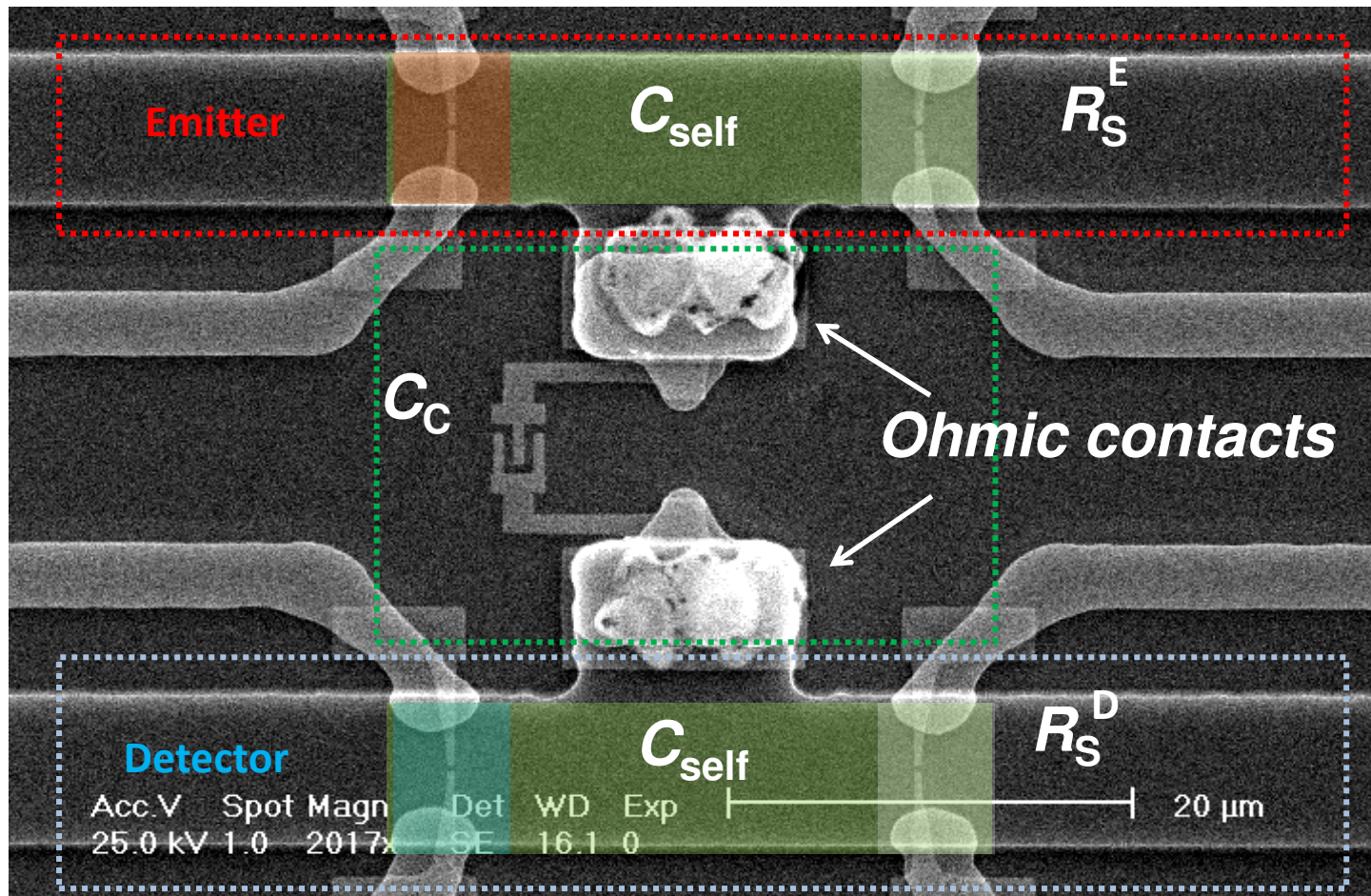
Figure 1: Device structure. **a** Scanning electron microscope view of the sample. Two independent circuit lines defined by wet-chemical etching of the 2DEG are coupled via the capacitance C_C . On the upper line are patterned two QPCs in series: the QPC emitter (in red), and the QPC series resistor (in white) tuned on a plateau. On the lower line, the QPC detector is colored in blue. **b**, Equivalent circuit. In red the emitter line is coupled via the coupling capacitance C_C to the detector line in blue. The self capacitances C_{self} have been added that model the capacitance of each line between the two QPCs to the ground.

Figure 2: Photocurrent measurement. **a**, Schematic representation of the experimental set up for the photocurrent measurement. The QPC emitter is excited by a sine wave function $V_{pp} \sim 460 \mu\text{V}$ at 174 Hz. The measurement of the photocurrent in the detector line is realized with a lock-in amplifier, with the excitation source as a reference signal. **b**, The photocurrent as a function of the total transmissions D_D (x-axis) and D_E (y-axis). On the upper graph is represented the photocurrent as a function of D_D (D_E tuned to 0.45). The right graph shows the photocurrent as a function of D_E (D_D tuned to 1.36).

Figure 3: PASN measurement. **a**, Schematic representation of the experimental set up for the PASN measurement. The QPC emitter being biased emits shot noise. Because of the capacitive coupling between the emitter and detector line, high frequency voltage fluctuations are transferred in the detector line, generating PASN. Shot noise measurements

are done by converting the current fluctuations into the voltage fluctuations across a RLC circuit, cooled at 300 mK using 3 MHz resonant frequency and 300 kHz typical bandwidth. Home made cryogenic amplifiers, with ultra low input voltage noise ($0.2 \text{ nV}/\sqrt{\text{Hz}}$) and located on the 3 K stage amplify the voltage fluctuations. Using fast acquisition card and Fast Fourier Transform, the current noise cross-correlation is computed in real time. **b**, Measured shot noise S_V as a function of dc voltage V_{ds}^D across the QPC detector, when the QPC series resistor is opened. **c**, Measured PASN S_V^{PASN} as function of the V_{ds}^E accross the QPC emitter. QPCs emitter and detector are tuned at $D_D=D_E=0.5$. Both series resistances are tuned on the first plateau.

Figure 4: Transmission dependence of the PASN. **a**, black dots: measured shot noise as a function of D_D for an opened series QPC together with our theoretical model (black solid line). red dots: same measurement with the series QPC tuned on a plateau. The non-zero value of the noise for $D_D = 1$ results from heating effect. In both cases $V_{ds}^D=100\mu\text{V}$. **b**, red dots: measured PASN as function of D_D for the series QPC tuned on the first plateau and a fixed $D_E \sim 0.5$ (theoretical prediction represented by a black solid line). The applied DC bias is $V_{ds}^E=6 \text{ mV}$.

a**b**